Simulation of Gb/s free space optical secure communication using interband cascade laser chaos

Han, Hong; Xu, Jiada; Cheng, Xumin; Jia, Zhiwei; Zhang, Jianguo; Shore, K. Alan

Optics Communications

DOI:
10.1016/j.optcom.2024.130424

Published: 05/03/2024

Peer reviewed version

Simulation of Gb/s free space optical secure communication using interband cascade laser chaos

Hong Han [1*], Jiada Xu[1], Xumin Cheng [1], Zhiwei Jia[1], Jianguo Zhang [1*], K. Alan Shore[2]

[1]*Key Laboratory of Advanced Transducers and Intelligent Control System, Ministry of Education, College of Electronic Information and Optical Engineering, College of Physics, Taiyuan University of Technology, Taiyuan 030024, China*

[2]*School of Electronic Engineering, Bangor University, Wales, LL57 1UT, UK*

**Corresponding author: hanhong@tyut.edu.cn; zhangjianguo@tyut.edu.cn*

Received Month Dec., 2023; accepted Month Feb., 2024; posted online Month Feb., 2024

We theoretically explore Gb/s message encryption in free space communications exploiting synchronized mid-infrared chaos from unidirectionally coupled interband cascade lasers (ICLs) with optical feedback. The achievable message encryption rate depends on the chaos bandwidth and relaxation frequency oscillation of the ICL which in turn, are determined by the bias current and the number of stages of the ICL. It is shown that message encryption rates up to 4 Gb/s may be obtained with bit error rate (BER) compatible with regular telecommunication systems requirements.

Keywords: *Chaos laser communication; Mid-infrared lasers; Interband cascade laser*

DOI: 10.1016/j.optcom.2024.130424

1. Introduction

Chaos secure communication offering high-level security and high transmission rates has been rapidly developed in relation to optical fiber links[1-6], where the key distribution rate is from 0.75Gb/s[3] to 2.25Gb/s[4], the encryption date rate reaches 60Gb/s[5] and achieves 100Gb/s[6]. In free space optical (FSO) communication, chaotic secure communication data rate began at a few Kbit/s and has approached Gb/s using the generation of broadband chaotic carrier for conventional communication wavelengths[7,8]. Considering atmospheric transmission characteristics and private communication in free space, the focus is on mid-infrared chaotic lasers, because in the 3-5μm band of the atmospheric transmission window has good atmospheric transmission characteristics, lower transmission losses than other bands, and is less susceptible to weather factors such as the presence of rain, dust, fog, and haze[9,10].

Interband cascade lasers (ICL) and quantum cascade lasers (QCL) are typical mid-infrared laser devices, which has been used to realize of order hundred Mb/s and Gb/s data rate in FSO communication[11-14]. Based on the atmospheric transmission characteristics of mid-infrared laser, rapid development of mid-infrared laser devices, and demand of high-speed communication, research into mid-infrared chaotic secure communication has occurred. QCL or ICL with external optical feedback, optical injection, and bias modulation have been investigated in parallel both experimentally and theoretically in order to obtain mid-infrared chaotic lasers[15-18]. To date, a 0.5Mbit/s transmission data rate has been achieved by unidirectionally coupled QCLs with external optical feedback operating in the chaotic regime, where the message is added to the bias current of the transmission QCL[19]. It is noted that the absence of high-frequency oscillations chaos limits the data rate. Fully-developed hyperchaos has been observed experimentally in ICLs subject to external optical feedback, where the electrical power spectrum exhibits a frequency span as broad as 2.0GHz[20]. Our previous theoretical research confirmed that ICL with external optical feedback, under certain conditions, can generate several GHz broadband chaos[21]. This opens a route towards high speed FSO secure communication.

In this paper, we demonstrate theoretically a Gb/s secure communication system based on chaos synchronization in ICLs. The bandwidth of the high-dimensional chaos is several GHz and synchronization correlation is above 0.9. A transmission rate at 4 Gb/s is achieved with an BER compatible with that of regular telecommunication systems.

2. Model

Figure 1 depicts chaos masking encoding and decoding techniques. In chaos masking, $C_T(t)$ is the chaos carrier which is generated by a master ICL with optical feedback. The binary code message $m(t)$, is added to the chaotic carrier and both are injected into the slave ICL. At the receiver, using chaos synchronization between the master and slave laser the decrypted message, $m(t)$, can be obtained using a low-pass filter operation: $m'(t)$ =LPF{$C_T(t)$+ $m(t)$- $C_R(t)$}, where $C_R(t)$ is the output of the slave ICL and LPF signifies that the recovered message is obtained using a fifth-order Butterworth low pass filter with a cut off frequency equal to the transmitted message bit rate.

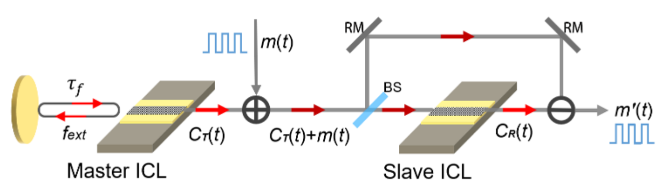

Fig. 1. Secure communication diagram of chaos masking.

In the simulations, modified Lang-Kobayashi rate equations are used[22,23]. In terms of the mean field slowly varying complex amplitudes of the electric field $E(t)$ and carrier number $N(t)$. The dynamics of the master ICL with optical feedback, is prescribed by the equations:

$$\frac{dE_m(t)}{dt}=\frac{1+i\alpha_H}{2}\left[m\Gamma_p v_g g-\frac{1}{\tau_p}\right]E_m(t)+ k_f E_m(t-\tau_f)\exp(-i\omega_m\tau_f) \quad (1)$$

$$\frac{dN_m(t)}{dt}=\eta\frac{I_m}{q}-\Gamma_p v_g g\left|E_m(t)\right|^2-\frac{N_m(t)}{\tau_{sp}}-\frac{N_m(t)}{\tau_{aug}} \quad (2)$$

The dynamical behaviour of the slave ICL is obtained using the equations:

$$\frac{dE_s(t)}{dt}=\frac{1+i\alpha_H}{2}\left[m\Gamma_p v_g g-\frac{1}{\tau_p}\right]E_s(t)+ k_i E_m(t-\tau_i)\exp(-i(\omega_m\tau_i+\Delta\omega t)) \quad (3)$$

$$\frac{dN_S(t)}{dt}=\eta\frac{I_s}{q}-\Gamma_p v_g g\left|E_s(t)\right|^2-\frac{N_s(t)}{\tau_{sp}}-\frac{N_s(t)}{\tau_{aug}} \quad (4)$$

where α_H is the linewidth enhancement factor, m is number of the cascade gain stage, Γ_p is the optical confinement factor per gain stage, v_g is the group velocity of light, g is the material gain per stage which is given by $g=a_0[N(t)-N_{tr}]/A$. A is the active area. τ_p is photon lifetime, and k_f is the feedback efficient which is given by $k_f=2C_l\sqrt{f_{ext}}/\tau_{in}$, where τ_{in} is the internal cavity round trip time, f_{ext} is the feedback strength which is defined as the power ration between the feedback light and the laser output, and C_l is an external coupling coefficient. The external coupling coefficient can be expressed as $C_l=(1-R)/2\sqrt{R}$, with R is the reflection coefficient of the laser front facet facing the external mirror. τ_f is the external cavity round trip time and η is the current injection efficiency. τ_{sp} is the spontaneous radiation lifetime and τ_{aug} is the Auger recombination lifetime. $k_i=2C_l\sqrt{r_{inj}}/\tau_{in}$ is the injection efficient which is defined as the power ration between the injection light and the laser output. I_m and I_s are the pump currents of the master and slave ICL respectively. ω_m is the angular frequency of master laser, $\Delta\omega=\omega_m-\omega_s$ where ω_s is the angular frequency of salver laser.

In the case of chaos masking, the message $m(t)$ is added to the chaotic carrier of the transmitter (master laser) which can be expressed as: $|E_m^{mod}(t)|=|E_m(t)|+hm(t)$, where h is the modulation depth that is masking coefficient, and $m(t)$ is the message which is on-off-keying data.

We follow common practice in using a correlation coefficient function to quantify the synchronization between the master and slave lasers[24,25]:

$$C(\Delta t)=\frac{\left\langle\left(I_m(t+\Delta t)-\left\langle I_m(t+\Delta t)\right\rangle\right)\cdot\left(I_s(t)-\left\langle I_s(t)\right\rangle\right)\right\rangle}{\sqrt{\left\langle\left(I_m(t+\Delta t)-\left\langle I_m(t+\Delta t)\right\rangle\right)^2\right\rangle\cdot\left\langle\left(I_s(t)-\left\langle I_s(t)\right\rangle\right)^2\right\rangle}} \quad (5)$$

where $I(t)=|E_m(t)|^2$ is the intensity time series, m and s stands for master ICL and slaver ICL. $I(t+\Delta t)$ contains time shift Δt with respect to $I(t)$, and $\langle\cdot\rangle$ stands for time averaging.

Table 1. ICL parameters used in the simulations.

Parameter	Symbol	Value
Cavity length	L	2mm
Cavity width	W	4.4μm
Group velocity of light	v_g	8.38×10^7m/s
Wavelength	λ_m	3.7μm
Active area	A	8.8×10^{-9}m^2
Facet reflectivity	R	0.32
Refractive index	n_r	3.58
Optical confinement factor	Γ_p	0.04
Stage number	m	10
Injection efficiency	η	0.64
Photon lifetime	τ_p	10.5ps
Spontaneous emission time	τ_{sp}	15ns
Auger lifetime	τ_{aug}	1.08ns
Threshold current	I_{th}	17.6mA
Differential gain	a_0	2.8×10^{-10}cm
Transparent carrier number	N_{tr}	6.2×10^7
Spontaneous emission factor	β	1×10^{-4}
Linewidth enhancement factor	α_H	2.2
Feedback strength	f_{ext}	0%~30%
Injection strength	r_{inj}	0%~80%
Feedback time delay	τ_f	2.4ns
Injection time delay	τ_i	2ns

In our simulations, the intrinsic parameters of the two lasers used are, first of all, assumed to be identical. As expected, the output of slave laser is highly consistent with that of master with the correlation coefficient (C) being close to 1, as shown in Fig. 2 (a-i) and (a-ii). It is noticed that master-slave synchronization cannot be achieved if the injection strength is relatively weak, as illustrated in Fig. 2(b-i) and (b-ii), where the injection strength, r_{inj}, is 10% and the correlation coefficient C is only 0.393.

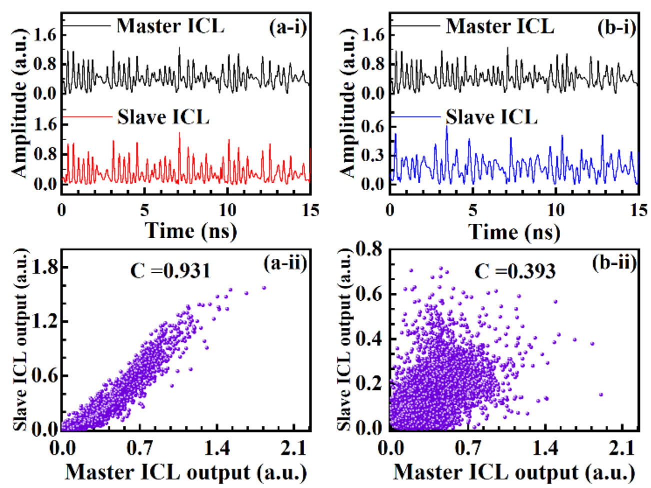

Fig. 2. From top to bottom: (i) temporal waveform and (ii) correlation plots of master and slave ICLs, where $r_{inj}=80\%$ for (a) and $r_{inj}=5\%$ for (b). Under conditions of $I_m=1.5I_{th}$, $I_s=1.2I_{th}$, f_{ext} =10%, $\Delta f=0$GHz.

3. Results

3.1. Chaotic synchronization

Chaos synchronization of the master and slaver lasers is the primary condition to achieve low BER chaos secure communications. In this section, we investigate the dependence of chaos synchronization on laser pump current, frequency detuning and ICL stage number.

Pump current effects on synchronization are presented in Fig. 3 (a) where f_{ext}=10%, r_{inj} = 80%. Once the pump current of the master laser exceeds that of the slave laser, the correlation coefficient reaches a relatively high value, as seen in the upper left sector of Fig. 3(a). A relatively high pump current of the master laser will enhance the injection light strength which increases the correlation coefficient. That is confirmed in Fig. 3(b), where $I_m = 1.5I_{th}$, $I_s = 1.2I_{th}$ and $r_{inj} \geqslant 24\%$, C $\geqslant$ 0.9 occupies a large region of the diagram. It has been reported in [20,21] that the feedback power ratio, f_{ext}, has an effect on the generation of chaos but we find that it has little influence on the correlation coefficient of master and slaver laser.

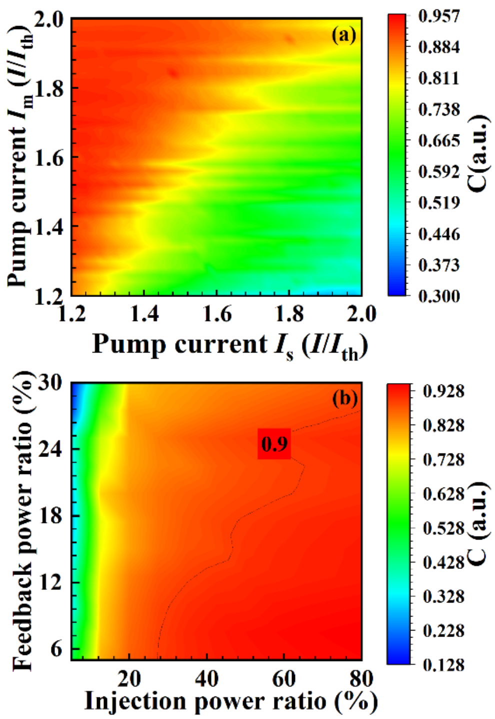

Fig. 3. For zero frequency detuning, correlation coefficient as a function of pump currents of master and slave ICLs (a) where f_{ext} =10%, r_{inj} = 80% and as a functions of feedback power ratio and injection power ratio (b) where $I_m = 1.5I_{th}$, $I_s = 1.2I_{th}$.

Attention is now given to another key parameter: the frequency detuning between the master and slaver lasers. From Fig. 4 it is seen that the correlation coefficient is further enhanced in some negative detuning regions also, increasing the injection power ratio, here r_{inj} is raised from 20% to 80%, causes the correlation coefficient to increase from 0.880 at Δf=-2GHz to 0.977 at Δf=-6GHz. For zero detuning, for these two power ratios, the correlation coefficients are respectively 0.860 and 0.940. This shows that in addition to strong injection power ratio, choosing an appropriate central wavelength of the slaver ICL is also important to obtain a high correlation coefficient for chaos secure communication.

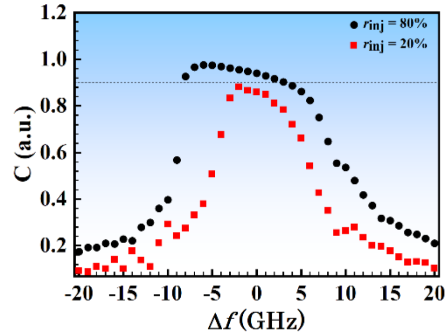

Fig. 4. Correlation as a function of frequency detuning, where $I_m = 1.5I_{th}$, $I_s = 1.2I_{th}$, $f_{ext} = 10\%$. Black circles and red squares present r_{inj}= 80% and r_{inj}= 20%, respectively.

Besides the zero detuning case shown in Fig. 3(a), we calculate frequency detuning effects on the correlation coefficient when the master and slave lasers are subject to different pump currents, as presented in Fig. 5(a). It is found that the upper left region of Fig. 5(a) corresponding high correlation coefficient values is enlarged and C can reach as high as 0.979. The relative higher correlation coefficient values required frequency detuning is shown in Fig. 5(b).

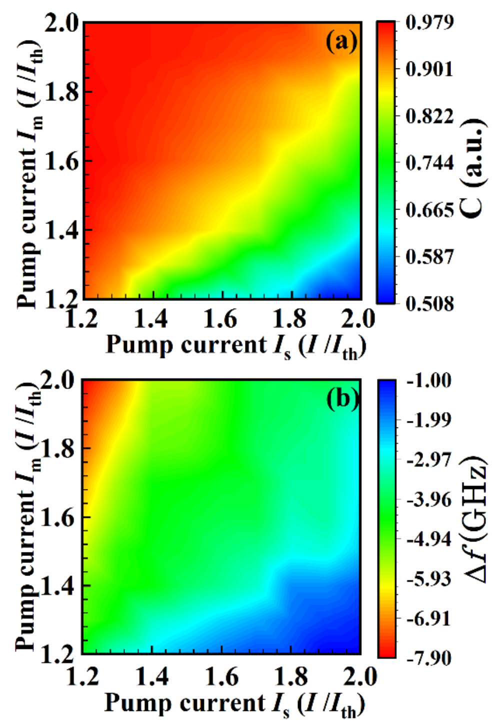

Fig. 5. Correlation coefficient as a function of pump currents of master and slave ICLs (a), and the required frequency detuning(b), where f_{ext} =10%, r_{inj} = 80%.

Figure 6 shows the required frequency detuning (black squares) for maintaining the maximum values of correlation coefficient (red circles) for same number of stages of master and slave ICLs. It is found that the correlation coefficient are almost constant when the number of stages of the master and slaver ICLs range from 2 to 20, and the required frequency detuning are the same.

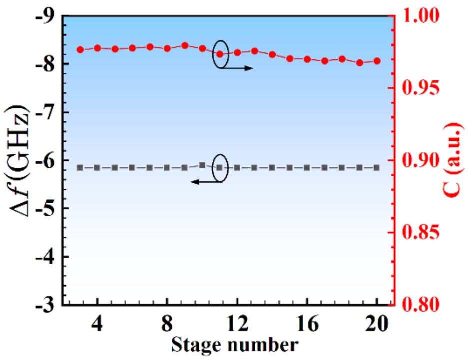

Fig. 6. Correlation coefficient value and corresponding frequency detuning under same stage number with Δf=-5.85GHz. I_m= 1.5I_{th}, I_s = 1.2I_{th}, f_{ext} =10%, r_{inj} = 80%.

3.2. Chaos masking

In this section, we present a typical encoding and decoding technique, based on above the mentioned chaotic synchronization and show that Gb/s message transmission rates can be achieved.

We find that the bandwidth of the RF spectrum of the chaotic carrier is broader than that of message, and then by choosing a relatively small modulation depth, the message can be hidden in the chaotic carrier. As presented in Fig. 7(a), when the pump current of master laser is set at 1.5 I_{th}, the chaos bandwidth can reach 4.37 GHz. We use here the conventional definition of chaos bandwidth of chaotic signals as the frequency span between the DC and the frequency range in which 80% of the energy is contained[26]. A 2 Gb/s message can be hidden in this chaotic carrier, as shown in Figure 7(b-iii).

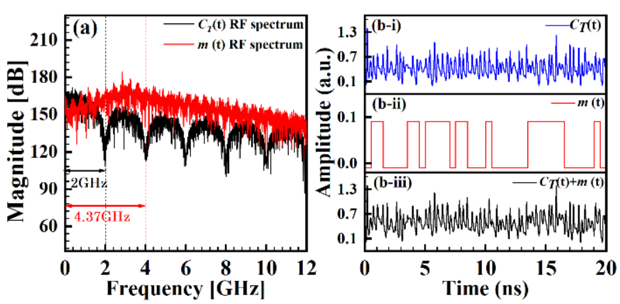

Fig. 7. (a) RF spectrum of chaotic carrier ($C_T(t)$) and message (m(t)); (b) temporal waveform of $C_T(t)$, m(t) and $C_T(t)$+$m(t)$. Under the condition of I_m = 1.5I_{th}, f_{ext} =10% and modulation depth h =0.1, message rate is 2Gb/s.

At the receiving terminal, the decrypted message can be obtained via $C_T(t)$+$m(t)$- $C_R(t)$, where $C_R(t)$ is from the slave ICL and has a high correlation coefficient with $C_T(t)$. Here, C=0.977. The corresponding decrypted result of 2Gb/s message is given by Figure 8, where the BER of message by chaotic decryption is 5.52×10^{-4} and it reaches 0.12 by direct decryption.

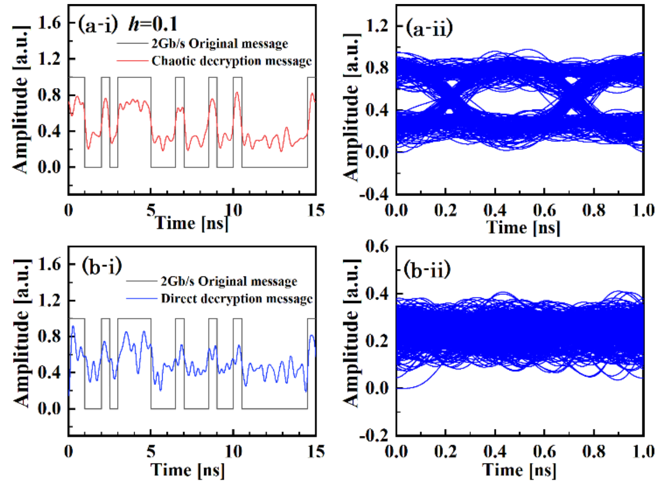

Fig. 8. Chaotic decryption (a) and direct decryption (b). (i): temporal waveform; (ii): eye-diagram. Under the conditions of I_m =1.5I_{th}, f_{ext}=10%, I_s=1.2I_{th}, r_{inj}=80%, Δf=-5.85GHz and modulation depth h = 0.1.

Figure 9(a) shows the BER performance of 2Gb/s message transmission rate under chaotic decryption (red circles) and direct decryption (black squares) versus modulation amplitude, respectively. It is seen that BER decreases with increasing modulation amplitude in both chaotic and direct decryption. For successful communication there is a requirement for the BER to be below 3.8×10^{-3}, which is the hard decision forward error correction (HD-FEC) threshold. This is met when the modulation amplitude is in the range 0.08 to 0.22. Once the modulation amplitude is larger than 0.22, the BER of direct decryption will be below the HD-FEC threshold which is as presented in black squares in Fig. 9(a). We also find that the correlation coefficient remains constant when modulation amplitude is below 0.25, as presented in Fig. 9(b).

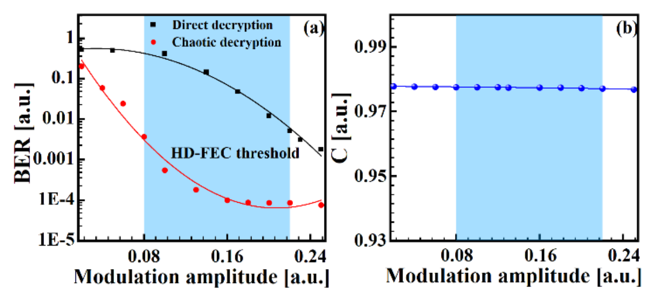

Fig. 9. BER performance of 2 Gb/s transmission rate under decryption as a function of modulation amplitude (a), and under the same conditions correlation coefficient versus modulation amplitude (b). Under conditions of I_m=1.5I_{th}, I_s=1.2I_{th}, f_{ext}=10%, r_{inj}= 80%, Δf= -5.85GHz.

By varying the frequency detuning or injection power ratio, we may obtain different correlation coefficient values to investigate correlation coefficient effects on the BER. Figure 10 shows the results of 1 Gb/s (black squares) and 2 Gb/s (red circles) message transmission rate under chaotic decryption versus correlation coefficient, where the modulation amplitude is 0.1. It is noticed that as the correlation coefficient increases, the BER gradually decreases. When the correlation coefficient reaches 0.90, the BER of the 1 Gb/s message is below the HD-FEC threshold. For the 2Gb/s message, the correlation coefficient should be at least 0.92 for the BER to be below the HD-FEC threshold. This shows that higher correlation coefficient value is an essential condition in order to obtain low BER or relatively high speed message rate.

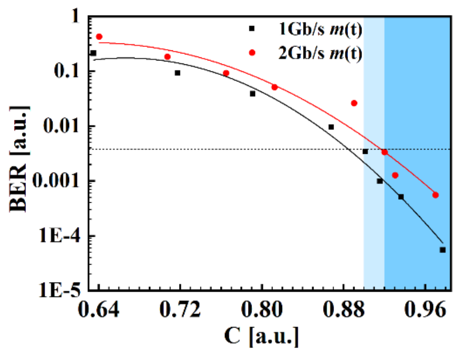

Fig. 10. BER performance of 1Gb/s (black squares)and 2Gb/s (red circles) transmission rate under decryption as a function of correlation coefficient. Under conditions of I_m =1.5I_{th}, I_s= 1.2I_{th}, f_{ext} = 10%, h = 0.1, r_{inj}= 80%, Δf= -5.85GHz.

We calculate the BER of chaotic decryption message as a function of the transmission rate as presented in Fig. 11. It is found that as the transmission rate increases, the BER increases, and when the rate reaches 2.3Gb/s, the BER is still below the HD-FEC threshold. In this case, the correlation coefficient is 0.97 which means that the synchronization is not perfect, therefore the BER will be above the HD-FEC threshold for the higher rate. The limitation on the transmission rate is that the message extraction will be less efficient when the message rate is comparable to the relaxation oscillation frequency of the laser. This has been reported in the case of chaos secure communication experiments using semiconductor lasers[25]. Of the two methods to increase transmission rate, choosing a laser with a relative high relaxation oscillation frequency is a much easier approach than seeking experimental means for further improving the correlation coefficient.

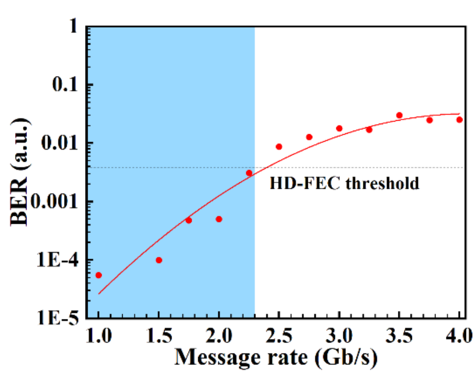

Fig. 11. BER performance under chaotic decryption as a function of transmission rate. Operation conditions of ICLs are same as Fig. 7 and Fig. 8, I_m =1.5I_{th}, I_s=1.2I_{th}, f_{ext}=10%, r_{inj}= 80%, h =0.1, Δf= -5.85GHz.

4. Discussion

To achieve higher transmission rate, one can increase the stage number or pump current of the ICLs which can both increase the relaxation oscillation frequency as shown in previous simulations[21]. Figure 12(a) and (b) respectively provide the decrypted results for 3Gb/s and 4Gb/s transmission rate. In the results shown in Fig. 8 the stage number was 10; here the number of stages is increased to 15 and 3Gb/s encryption is realized. We find that the rate can be further improved to 4Gb/s, with only a slight increase of the pump current of the master and slave lasers to 1.7I_{th} and 1.3I_{th} respectively.

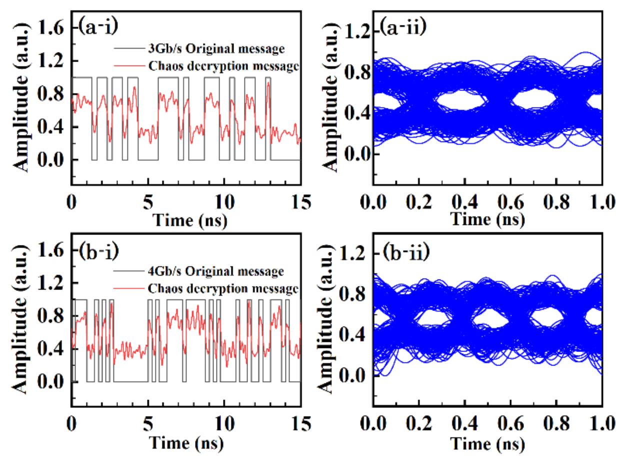

Fig. 12. Chaotic decryption results of 3Gb/s (a) with I_m =1.5I_{th} I_s=1.2I_{th}, f_{ext}=10%, r_{inj}=80%, m_m = m_s=15, h =0.1, Δf= -5.85GHz, C=0.97, BER=1.20×$10^{-3}$and 4Gb/s (b) with I_m=1.7I_{th} I_s= 1.3I_{th}, f_{ext} =15%, r_{inj} =80%, m_m = m_s=15, h =0.1, Δf = -5.50GHz, C =0.96, BER=1.81×10^{-3}. (i): temporal waveform; (ii): eye-diagram.

5. Conclusions

Theoretical investigations have been undertaken of the requirements for successful secure free-space optical communications using chaotic ICLs. With increase of pump current, injection pow ratio as well as ICL stage number, we obtain high-quality synchronization and broadband chaotic laser carrier. Based on this, we encrypt a 4Gb/s message by chaos masking. Prospects for transmission rates at several Gb/s are indicated offering a stimulus for an experimental demonstration of this communication scheme.

Acknowledgement

This work was supported by Natural Science Foundation of Shanxi Province, grant number 20210302123185 and 20210302124038, and Research Project Supported by Shanxi Scholarship Council of China, grant number 2021-032, and National Natural Science Foundation of China, grant number 61741512, and the Fund for Shanxi "1331 Project" Key Innovative Research Team.

References

1. M. Sciamanna, K.A. Shore, Physics and applications of laser diode chaos, Nat. Photonics 9 (3) (2015) 151-162.
2. N. Jiang, A.K. Zhao, C.P. Xue, J.M. Tang, and K. Qiu, Physical secure optical communication based on private

chaotic spectral phase encryption/decryption, Opt. lett. 44 (7) (2019) 1536-1539.
3. H. Gao, A.B. Wang, L.S. Wang, Z.W. Jia, Y.Y. Guo, Z.S. Gao, L.S. Yan, Y.W. Qin, and Y.C. Wang, 0.75 Gbit/s high-speed classical key distribution with mode-shift keying chaos synchronization of Fabry-Perot lasers, Light Sci. Appl. 10 (1) (2021) 172.
4. L.H. Mo, A.B. Wang, Y.H. Sun, J.P. Xu, Y.H. Zhang, X.H. Zhang, Y.W. Qin, Y.C. Wang, Physical-layer key distribution based on commonly-driven laser synchronization with random modulation of drive light, Opt. Express 31 (26) (2023) 42838-42849.
5. Y.Q. Wu, H.W. Luo, L. Deng, Q. Yang, X.X. Dai, D.M. Liu, and M.F. Cheng, 60 Gb/s coherent optical secure communication over 100 km with hybrid chaotic encryption using one dual-polarization IQ modulator, Opt. lett. 47 (20) (2022) 5285-5288.
6. Y.H. Xie, Z. Yang, M.Y. Shi, Q.B. Zhuge, W.S. Hu, and L.L. Yi, 100 Gb/s coherent chaotic optical communication over 800 km fiber transmission via advanced digital signal processing, Advanced Photonics Nexus 3 (1) (2024) 016003
7. N.F. Rulkov, M.A. Vorontsov, and L. Illing, Chaotic free-space laser communication over a turbulent channel, Phy. Rev. Lett. 89 (27) (2002) 277905.
8. Y.Q. Zhang, M.F. Xu, M.B. Pu, Q. Chen, M.J. Zhou, S.C. Chen, K. Qiu, N. Jiang, and X.G. Luo, Experimental demonstration of an 8-Gbit/s free-space secure optical communication link using all-optical chaos modulation, Opt. Lett. 48 (6) (2023) 1470-1473.
9. Y.L. Su, W. Wang, X.H. Hu, H. Hu, X.N. Huang, Y.S. Wang, J.H. Si, X.P. Xie, B. Han, H. Feng, Q. Hao, G.S. Zhu. T. Duan, and W. Zhao, 10 Gbps DPSK transmission over free-space link in the mid-infrared, Opt. Express 26 (26) (2018) 34515-34528.
10. A. Soibel, M.W. Wright, W.H. Farr, S.A. Keo, C.J. Hill, R.Q. Yang, and H.C. Liu, Midinfrared interband cascade laser for free space optical communication, IEEE Photonics Technol. Lett. 22 (2) (2009) 121-123.
11. P. Corrigan, R. Martini, E.A. Whittaker, and C. Bethea, Quantum cascade lasers and the Kruse model in free space optical communication, Opt. Express 17 (6) (2009) 4355-4359.
12. O. Spitz, P. Didier, L. Durupt, D.A. Díaz-Thomas, A.N. Baranov, L. Cerutti, and F. Grillot, Free-space communication with directly modulated mid-infrared quantum cascade devices, IEEE J. Sel. Top. Quantum Electron. 28 (1) (2021) 1-9.
13. X.D. Pang, O. Ozolins, L. Zhang, R. Schatz, A. Udalcovs, X.B. Yu, G. Jacobsen, S. Popov, J.J. Chen, and S. Lourdudoss, Free - space communications enabled by quantum cascade lasers, Phys. Status. Solidi (a) 218 (3) (2021) 2000407.
14. X.D. Pang, R. Schatz, M. Joharifar, A. Udalcovs, V. Bobrovs, L. Zhang, X.B. Yu, Y.T. Sun, G. Maisons, M. Carras, S. Popov, S. Lourdudoss, and O. Ozolins, Direct modulation and free-space transmissions of up to 6 Gbps multilevel signals with a 4.65-μ m quantum cascade laser at room temperature, J. Light. Technol. 40 (8) (2022) 2370-2377.
15. O. Spitz, L. Durupt, and F. Grillot, Competition between Entertainment phenomenon and chaos in a quantum cascade laser under strong optical reinjection, Photonics 9 (1) (2022) 29.
16. X.G. Wang, B.B. Zhao, Y. Deng, V. Kovanis, and C. Wang, Nonlinear dynamics of a quantum cascade laser with tilted optical feedback, Phys. Rev. A 103 (2) (2021) 023528.
17. M.R. Zhao, G.Q. Xia, K. Yang, S.M. Liu, J.Q. Liu, Q.P. Wang, J.L. Liu, and Z.M. Wu, Nonlinear dynamics of mid-infrared interband cascade lasers subject to variable-aperture optical feedback, Photonics 9 (6) (2022) 410.
18. Z.W. Jia, L. Li, Y.Y. Guo, A.B. Wang, H. Han, J.C. Zhang, P. Li, S.Q. Zhai, and F.Q. Liu, Periodic and chaotic oscillations in mutual-coupled mid-infrared quantum cascade lasers, Chinese. Phys. B 31 (10) (2022) 100505.
19. O. Spitz, A. Herdt, J.G. Wu, G. Maisons, M. Carras, C.W. Wong, W. Elsäßer, and F. Grillot, Private communication with quantum cascade laser photonic chaos, Nat. Commun. 12 (1) (2021) 3327.
20. Y. Deng, Z.F. Fan, B.B. Zhao, X.G. Wang, S.Y. Zhao, J.G. Wu, F. Grillot, and C. Wang, Mid-infrared hyperchaos of interband cascade lasers, Light Sci. Appl. 11 (1) (2022) 7.
21. H. Han, X.M. Cheng, Z.W. Jia, and K.A. Shore, Nonlinear dynamics of interband cascade laser subjected to optical feedback, Photonics 8 (9) (2021) 366.
22. R. Lang, K. Kobayashi, External optical feedback effects on semiconductor injection laser properties, IEEE J. Quantum Electron 16 (3) (1980) 347-355.
23. Y. Deng, C. Wang, Rate equation modeling of interband cascade lasers on modulation and noise dynamics, IEEE J. Quantum Electron 56 (2) (2020) 1-9.
24. N. Jiang, A.K. Zhao, S.Q. Liu, C.P. Xue, and K. Qiu, Chaos sychronization and communication in closed-loops semiconductor lasers subject to common chaotic phase-modulated feedback, Opt. Express 26 (25) (2018) 32404-32416.
25. L.S. Wang, Y.Y. Guo, D.M. Wang, Y.C. Wang, ang A.B. Wang, Experiment on 10-Gb/s message transmission using an all-optical chaotic secure communication system, Opt. Commun. 453 (2019) 124350.
26. F.Y. Lin, J.M. Liu, Nonlinear dynamical characteristics of an optically injected semiconductor laser subject to optoelectronic feedback, Opt. Commun. 221 (1-3) (2003) 173-180.